Published in final edited form as:
J Mol Biol. 2008 December 5; 384(1): 219–227. doi:10.1016/j.jmb.2008.09.021.

Molecular basis for Proline- and Arginine-Rich Peptide inhibition of proteasome

Asokan Anbanandam[1], **Diana C. Albarado**[1], **Daniela C. Tirziu**[2], **Michael Simons**[2], and **Sudha Veeraraghavan**[1]

[1]Department of Biochemistry & Molecular Biology, University of Texas Health Science Center at Houston, Medical School, 6431 Fannin, St., Houston, TX 77030

[2]Angiogenesis Research Center and Section of Cardiology, Departments of Medicine and Pharmacology and Toxicology, Dartmouth-Hitchcock Medical Center, Dartmouth Medical School, Lebanon, New Hampshire 03755

Summary

PR39, a naturally occurring and cell-permeable proline-and arginine-rich peptide, blocks the degradation of IκBα hereby attenuating inflammation. It is a non-competitive and reversible inhibitor of 20S proteasome. To identify its basis of action, we used solution NMR spectroscopy and mutational analyses of the active fragment, PR11, which identified amino acids required for human 20S proteasome inhibiting activity. We then examined PR11 mediated changes in the expression of NF-κB-dependent genes *in situ*. The results provide prerequisites for proteasome inhibition by PR-peptides providing a powerful new tool to investigate inflammatory processes. These findings offer new leads in developing drugs to treat heart diseases or stroke.

Keywords

Proteasome inhibition; proline-and-arginine rich peptides; NF-κB; NMR

INTRODUCTION

PR39 is a cathelin-like ‘proline-and-arginine rich peptide’ (PR-peptide) that was originally isolated from pig intestine for its antimicrobial property1; 2. PR39 and its homologs are secreted by macrophages and found in the wound fluid of many animals as well as along the border of acute myocardial infarction3. Secreted as a prepropeptide, the mature 39 amino acid C-terminal polypeptide chain (PR39) is produced by rapid cleavage of a canonical leader sequence4.

Recent studies show that PR39 stimulates angiogenesis *in vitro* and *in vivo*. Transgenic expression in cardiac myocytes results in increased vessel numbers and reduced coronary resistance5 and myocardial hypertrophy6. These effects appear to derive from the inhibition of HIF-1α degradation, which results in increased VEGF expression. Interestingly, PR39 also increased the expression of FGFR1 and syndecan-4, another FGF receptor7; 8,

*Correspondence to*Sudha.Veeraraghavan@uth.tmc.edu, Tel: 713-500-6089, Fax: 713-500-0652.

suggesting that PR39 may also induce angiogenesis *via* the FGF pathway. Furthermore, PR39 treatment reduces tissue injury in inflammatory states by reducing the influx of white blood cells and by decreasing expression of NF-κB -dependent expression of adhesion molecules on endothelial cell surface9; 10. PR39 appears to function by selectively inhibiting degradation of HIF-1α and the NF-κB inhibitor, IκBα10.

Non-lysosomal degradation of cellular proteins occurs by the action of E1, E2 and E3 enzymes that result in the tetra-ubiquitinylation of target proteins and their proteolysis by the enzymatic activities residing within the central chamber of the 20S proteasomes. Ubiquitin and ubiquitin-like proteins are responsible for regulating numerous cellular pathways including the cell division cycle, transcription, protein sorting in the secretory pathway, membrane protein transport, endocytosis, nuclear transport, and signal transduction, by marking substrate proteins for degradation by proteasomes. The identification and analyses of inhibitors of proteasome are, therefore, of immense value to treat a variety of diseases such as cancer, autoimmune diseases, muscle wasting, and inflammation 11; 12; 13; 14; 15. One most successful example of proteasome-based drug is the boronate, bortezomib (Velcade^{Tm} or PS-341) 16; 17.

Cylindrical 20S proteasomes of eukaryotes, at approximately 700 kD mass, are composed of two heptameric inner rings of β-subunits and two heptameric outer rings of α-subunits. The chymotrypsin-like, PGPH (caspase)-like, and trypsin-like activities of proteasomes reside within the beta subunits18; 19. The α-subunits are not known to possess proteolytic activities. It is, therefore, remarkable that binding of PR-39 to the α7 subunit of 20S proteasome is able to selectively inhibit proteolytic degradation of some polypeptide chains, such as IκBα 10. This interaction produces a gross structural change in 20S proteasome20. However, no high resolution structures of the complex are available, presumably due to the reversible nature of the interaction. Therefore, properties of PR39 that are necessary for inhibition of 20S proteasomes remain unknown.

A peptide comprising the first eleven residues of PR39, namely PR11, is also able to inhibit the 20S proteasome20. Using site-specific mutagenesis and solution NMR spectroscopy, here, we identify the conformational requirements for PR11 activity against 20S proteasome. We find that to effectively inhibit 20S proteasome, PR11 requires at least two positively charged residues (Arg or Lys) at the N-terminus and hydrophobic residues at the C-terminus. Importantly, properties of PR11 required to inhibit 20S proteasome *in vitro* are also required to alter gene expression along the NF-κB pathway. We discuss various models that explain PR11 activity.

RESULTS

NMR spectroscopy of PR11

To establish conformational requirements of active PR11, we examined PR11 using homonuclear solution NMR spectroscopy. PR11 contains five arginines and four prolines. Severe overlap in the beta and gamma proton chemical shifts of these residues presented a significant challenge to spin system identification, resonance assignment, and conformational analysis by NMR with data taken using a 800 MHz spectrometer. To overcome these challenges, we used TOCSY and NOESY spectra of wild type and various alanine substituted PR11 to identify each spin system and to make sequence-specific assignments (Table I). The finger print region of the NOESY spectrum of PR11 is shown in Fig. 1 (Left panel). Sequential connectivities between of alpha proton (H_α) of the any given residue (i) and the amide proton (HN) of the following residue (i+1) were used to establish residue specific assignments. Such NOE contacts were not observed for the first three

arginines, presumably due to fast relaxation. The intervening Pro residues lack a backbone amide proton, and hence, the connectivity is broken four times.

The four prolines are located at positions 4, 6, 7, and 10. The cyclic nature of the proline side chain restricts rotation about the Xaa-Pro bond and constrains it to either *cis* or *trans* configuration 21; 22. Peptides containing prolines can, therefore, exist in multiple conformations. Furthermore, when preceded by branched chain or bulky amino acids, the population of *cis* conformer increases23; 24. Thus, with its Pro-Pro and Leu-Pro bonds, PR11 is expected to consist of populations in which one or more *cis* conformers exist. If so, we would expect to see multiple sets of NMR cross-peaks corresponding to each of these conformers. As expected, the NMR spectrum of PR11 (Fig. 1) shows one set of cross peaks corresponding to the major conformer at about 80% concentration and at least one minor conformer. In addition, amide protons of Arginine 5 and Leucine 9 each resonate at two distinct chemical shifts. We also observed weak NOE cross peaks between $C^{\alpha}H$ (i) to $C^{\alpha}H$ (i+1) confirming the presence of minor conformers containing Xaa-Pro *cis* bonds. However, strong NOE cross peaks between $C^{\alpha}H$ (i) to Pro $C^{\delta}H_2$ (i+1) (Fig. 1, right panel) confirmed that the major conformer of the peptide consists of the all-*trans* conformer.

The amide region of the NOESY spectrum of PR11 shows that NOEs between amides of adjacent residues are observed only for Tyr8 and Leu9 (Supplementary data, Fig. S1). Also, weak NOEs are detected between the amide protons of Leu9 and the $C_{\delta}H$ ring proton of Tyr8, consistent with spatial and sequence proximity of these residues.

PR11 contains one aromatic residue, Tyr8. Its Hδ and Hε side chain protons resonate at 7.13 and 6.84 ppm (Table I). Nuclear Overhauser Effect (NOE) correlations to these peaks from various residues of PR11 provide unique signatures for wild type and each mutant peptide (Supplementary data, Fig. S2). For instance, cross-peaks corresponding to Tyr8' (a minor conformer) Hδ that resonate at 6.7 ppm disappear in the Pro7Ala mutant. Furthermore, cross peaks to Tyr8' Hδ are very weak in the Pro6Ala mutant, and several cross peaks to the major and minor conformer are missing in the Pro10Ala mutant. These data indicate that Pro7, Pro6, and Pro10 produce the minor. conformers in PR11. In the case of Pro4Ala mutant, certain cross peaks to the major conformer are weaker or missing, consistent with loss of side chain protons of the proline. These results suggest that Pro4 and Pro10 provide conformational rigidity to the molecule.

In general, small peptides like PR11 do not contain regular secondary structural elements. Hence, it is not surprising that the alpha proton chemical shifts of PR11 deviate little from random coil values except due to local sequence variations, such as when a residue is preceded by a proline. NMR-based model of the trans PR11 peptide (Supplementary data, Fig. S3 and Table S1) confirms this prediction and only the backbone and side chains of residues, Pro4 and Tyr8 are relatively well-defined.

20S-inhibitory activity of PR11 and its mutants

To determine whether the major, all-trans conformer of PR11 is the active form and to establish the chemistry responsible for PR11 activity, we examined the inhibition of chymotrypsin-like activity of human 20S proteasome by PR11 and its site-specific mutants.

AAA-PR11, in which the first three arginines are mutated to alanines, does not inhibit IκBα degradation by 20S proteasome9. To determine whether the PR11 activity was specific to the presence of arginine residues or simply requires positive charges at the N-terminus, we replaced each of the three arginines with a lysine. The replacement of any one of the first three arginines of PR11 with lysine alters the activity only slightly and the I50 remains in the range of ~0.5–0.8 μM (Fig. 2, Table II). This is not surprising. as Arg->Lys is a

conservative replacement and the positive charge on the side chains are retained in each of these mutants. However, replacement of all three arginines with lysines (KKK-PR11) makes the peptide less active (I50 to 2.7 μM). It suggests that PR11 interaction with 20S proteasome involves not only electrostatic forces but perhaps also hydrogen bonding since hydrogen-bonding patterns of lysine and arginine are different.

To establish that positively charged residues are necessary for PR11 activity, we replaced each arginine with alanine. The mutant peptides have activities similar to the KKK peptide even though only one arginine is mutated to alanine, indicating that charge-charge interactions play an important role in recognizing 20S proteasome. To then examine whether all three arginines are necessary for the activity or just any two would suffice, we mutated pairs of arginines in the first three residues. Strikingly, the I50s for double mutants are in between those of single mutations and the triple (AAA) mutation. Thus, the contribution of the arginines to the 20S inhibiting activity of PR11 is additive. Like the single alanine mutations at positions 1–3, the Arg5Ala mutant shows lower activity indicating it also contributes similarly to PR11 activity.

To determine whether the active form of PR11 consists of a *cis* bond, each Proline was mutated to an alanine. Ala mutants of residues Pro6, Pro7, or Pro10 had little to no effect on PR11 activity and we conclude that proline *cis-trans* isomerization about the Arg5-Pro6, Pro6-Pro7, or Leu9-Pro10 bonds do not contribute noticeably to PR11 activity. Pro4Aala mutant shows increased I50 (5 μM). It suggests that the *cis* conformer at the Arg3-Pro4 bond may contribute to the 20S inhibiting activity of PR11. However, since the mutation does not abolish 20S proteasome inhibiting activity (compare with AAA-PR11), it is likely that presence of Pro4 enhances PR11 activity by providing structural rigidity or by limiting spatial sampling by N-terminal residues of PR11 as also indicated by results from our NMR experiments.

A peptide containing the N-terminal 8 residues of PR11 (PR8, RRRPRPPY) does not inhibit 20S proteasome suggesting that Leu9 is important20. We asked if this is because hydrophobicity of Leu9 is necessary interactions with 20S proteasome. To test this, we replaced Leu9 with glycine. We chose Gly over Ala, since Ala is also hydrophobic. Unexpectedly, the Leu9Gly mutant is more active (I50 of 0.14 μM) than wild type PR11 (I50 of 0.81 μM), indicating that Leu9 does not determine the 20S-inhibiting or binding activity of PR11 and that a bulky hydrophobic residue is not preferred at position 9. The results imply that Leu9Gly mutation converts the *cis* Leu9-Pro10 to *trans* Gly9-Pro10, which is the favored active conformation. One explanation why PR8 is inactive is that although Leu9 and Pro10 are not essential for the activity, perhaps Arg11 is. So, we made an Arg11Ala mutant. This mutant is also quite active with I50 for 20S inhibition of 0.69 μM. These results show that although any one of the three residues at the C-terminal end is dispensable, together these are necessary for either recognition of or selecting the conformation associated with the selective inhibition of 20S proteasome.

Tyr8 is a particularly interesting component of PR11. It consists of multiple chemical characteristics – a hydroxyl, aromatic ring, and hydrophobicity. So, are all of these properties essential for PR11 activity? We hypothesized that if the electronegative hydroxyl group is necessary for 20S binding or inhibition, mutation of Tyr8 to Glu would improve PR11 activity, whereas if the aromatic or hydrophobic interactions are more important, mutation to Glu would impair PR11 activity but mutation to another hydrophobic residue lacking the hydroxyl group (Phe) would leave PR11 activity unaltered. We find that Tyr8Glu mutation worsens the I50 (2.4 μM), whereas the double-mutant Lys1Glu8 has a significantly increased I50 (6.3 μM). In comparison, Lys1 mutation alone shows a slight improvement with I50 at 0.6 μM. That Lys1Glu8 is a worse inhibitor of 20S, once again,

reiterates that mutating multiple key residues compounds the adverse effects with regard to 20S recognition or inhibition. We also designed a Glu8Trp12 mutant to help determine peptide concentration using the UV absorbance properties of the tryptophan, in mutants lacking tyrosine. This peptide behaves much the same as the Glu8 mutant indicating that the addition of Trp12 does not significantly alter PR11 activity. To confirm the latter, we also designed a control in which Trp 12 is added to the normal PR11. Surprisingly, Trp12 PR11 is actually more active than PR11 (Table III) and is, within errors, as active as full-length PR39 (Table II). Thus, the adverse effects of Glu8 carboxyl overpower the benefit of Trp12 and we conclude that the hydroxyl group of Tyr8 does not play a role in PR11 activity. As for the hydrophobic mutations – Ki of Tyr8Ala is nearly half of PR11 (Table III) and that of Tyr8Phe, which simply removes the hydroxyl group, is only about two-fold greater than that of PR11. Thus, our efforts to identify the key chemistries in PR11 have also led to the design of more active PR11 variants, namely Ala8 PR11 and Trp12 PR11.

PR11 regulation of NF-κB-related gene expression

NF-κB is a key component of the inflammatory pathway. Previously, we showed that PR39, which crosses cell membranes readily 4; 25; 26, acts as an anti-inflammatory agent by inhibiting degradation of IκBα, and thereby inhibits NF-κB activity 9; 10. This results in down-regulation of NF-κB-dependent gene expression of the vascular cell adhesion molecule, VCAM-1 10. We reasoned that, like PR39, PR11 and its mutants that inhibit 20S proteasome activity *in vitro* would down-regulate NF-κB-dependent gene expression of VCAM-1. Indeed, in the presence of PR11 and several of its mutants, induction level of VCAM-1 isoforms (110kDa and 100kDa) was considerably reduced, on average by 50% relative to controls lacking PR-peptides. This indicates that NF-κB activity is impaired (Fig. 3A and B). Consistent with these results, the AAA PR11 mutant does not significantly reduce VCAM-1 induction, indicating that this peptide is inactive *in vivo* as well as *in vitro*. The Ala1Glu8 and Lys1Glu8 mutants, and to a lesser extent, the Ala1 and Ala3 mutants are less effective in down-regulating VCAM-1 expression (Fig. 3B). Thus, PR39 and PR11 are most active *in situ* and *in vitro* and AAA-PR11 is least active. Other mutants with intermediate activities in vitro also show intermediate activities *in vitro*. These findings suggest that the *in situ* effects of PR11 stem largely from its ability to inhibit proteasomes.

DISCUSSION

The prototypical NF-κB, p50/p65 heterodimer, is the most abundant and biologically active member of the mammalian Rel/NF-κB family of inducible transcription factors. Nuclear localization signal comprising the C-terminal 13 residues of NF-κB is masked by binding to IκBα, an ankyrin repeat domain-containing protein, impeding nuclear localization of NF-κB. Also, a nearly 180° movement of the N-terminal domain of p65 upon complexation with IκBα hinders DNA binding. Thus, the expression of numerous genes involved in immune and inflammatory responses, cell proliferation, and apoptosis that are under the control of NF-κB is regulated by IκBα binding. IκBα itself is rapidly turned over in cells27. PR11 inhibits IκBα degradation resulting in high levels of ubiquitinated IκBα retained in cells10 and is associated with down-regulation of NF-κB-dependent expression of VCAM-1.

In cells, proteasomes exist in equilibrium between the fully assembled, 26S, and partially disassembled, 20S+19S, subunits. Proteasomal degradation of cellular proteins can proceed directly using the 20S subunit or require unfolding first using the 19S lids of 26S proteasome. It is possible that IκBα, with its loose fold28, could be degraded by 20S as well as 26S proteasomes, contributing to its rapid turnover. How then, does PR11 influence the turnover rate of IκBα? We previously established that PR39 binds to the N-terminal segment of the α7 subunit of 20S proteasome 10. Here, we propose that PR11 interacts with

20S proteasome based on complementarity between the surfaces of PR11 and N-terminal region of α7 subunit. There are at least two consequences of this binding. *First*: the entryway into the central chamber is occluded disallowing entry IκBα for degradation 20. If this were the only mechanism, then the degradation of all protein substrates of 20S proteasome would be reduced just like IκBα. However, total cellular protein degradation is not greatly inhibited by the presence of PR11 compared to other inhibitors like MG132 10. This may be due to reversible binding of PR11. *Second*: more recently, the isolated heptameric C-terminal peptide of the 19S ATPase containing the ϕYX motif (for e.g., Leu-Tyr-Ala and Leu-Tyr-Trp) was found to be capable of inducing gate opening in 20S proteasomes29. Since proline and leucine are isosteres, PR11 with its Pro-Tyr-Leu and its N and C-terminal Arg may bind to the α7 subunit, in a manner analogous to that by PAN C-terminal peptide to open the 20S gate and interfere with assembly of the 19S lid. This is consistent with the atomic force microscopic evidence demonstrating a partially open 20S proteasome when complexed with PR11. The consequences of such an interaction would be two-fold: (a), proteins requiring unfoldase activity in the 19S lid may not be degraded by PR11-bound 20S. (b), since the peptide associates with 20S proteasome in a reversible manner, the inhibition to degradation by 20S would be temporary such that the net reduction in cellular protein turnover would be small. This model is also consistent with our earlier observations that PR11 reduces proteasome mediated total cellular protein degradation but does not abolish it.

Alternatively, PR11-bound 20S presents a new surface to incoming IκBα which masks part of the original 20S surface at the mouth. It is conceivable that interactions between IκBα and α7 subunit of 20S proteasome improve lifetime of the IκBα/20S complex. If so, IκBα might suffer from unproductive encounters with the altered surface of 20S when bound by PR11, resulting in inhibition of its proteolysis. That some other proteins could also favorably interact with the new surface cannot be discounted, and may explain the overall reduction in the degradation of cellular proteins10. In reality, one or more of these scenarios may determine the mechanism of action of PR-peptides.

In a most exciting finding, we have identified not only the residues critical for PR11 action, but also discovered new, more potent, PR11-based 20S inhibitors. Furthermore, the manner in which PR-peptide activity affects IκBα degradation closely corresponds to the extent by which 20S proteasome activity is inhibited *in vitro*. Similarities the *in situ* and *in vitro* effects makes these peptides excellent targets for further development of anti-inflammatory drugs targeting the NF-κB pathway. Since PR11 inhibition of IκBα degradation results in high levels of ubiquitinated IκBα to be retained in cells10 it remains to be seen whether expression of upstream genes, including NF-κB itself, are altered by PR-peptides.

MATERIALS AND METHODS

Proline-and-arginine rich peptides

The amino acid sequence of chemically synthesized PR-peptide used the porcine PR39 sequence (NH2-**RRRPRPPYLPR**PRPPPFFPPRLPPRIPPGFPPRFPPRFP-COOH). Synthetic PR39, PR11 (bold typeface in PR39 sequence), and AAA-PR11 were purchased from C S Bio Inc. (San Carlos, CA) or Genemed Biotechnologies, Inc. (South San Francisco, CA). All other peptides were purchased from the Tufts University Core Facility (Boston, MA). All peptides used in this study were HPLC-purified and dissolved in phosphate-buffered saline. Peptide concentrations were determined using the molar extinction co-efficient, at 280 nm, of the single tyrosine (1280 M^{-1} cm^{-1}) or tryptophan (5700 M^{-1} cm^{-1}).

Determination of Enzymatic Activity

Mammalian (Human) 20s Proteasome was purchased from Boston Biochem (Cambridge, MA). The substrate, N-succinyl-LLVY-AMC and negative control, Lactacystin, were purchased from Sigma. The chymotrypsin-like (ChT-L) peptidase activity was measured using the N-Succinyl-LLVY-AMC substrate (Sigma, MO) as described earlier20. Activity was determined by measuring the amount of a fluorescence observed upon release of the MCA group after a 1 h incubation at 37 °C in 50 mM Tris.HCl buffer at pH 7.5 containing 0.03% SDS (Supplementary data, Fig. S4). Inhibition by PR-peptide was measured after a 15 minute pre-incubation at 37 °C of each peptide with 20S proteasome, followed by the addition of the substrate and the one hour incubation. I50 values correspond to concentration of PR-peptide required for 50% inhibition of 20S activity and were determined from plots of activity vs. PR-peptide concentration by least-squares curvefitting of the data using the equation:

$$\log (y/(1-y)) = n \log [\text{PR} - \text{peptide}] - n \log I50, \quad \text{Eq. 1}$$

where, n corresponds to fractional occupation of PR-peptides on 20S. Curve-fitting was performed using Origin Ver. 6.1 (Microcal, MA).

Ki determinations – Human 20S proteasome (5nM) was incubated in 50 mM Tris.HCl buffer, pH 7.5, containing 0.03% SDS and 0, 75, or 150 nM PR-peptide. Kinetic reactions, at 37 °C, were initiated by the addition of substrate (Suc-LLVY-AMC) at 20–100μM. Data was fit to the Michaelis-Menton equation using non-linear least-squared curve-fitting routine in Origin Ver. 6.1 (Microcal, MA). The reactions followed reversible non-competitive kinetics (Supplementary data, Fig. S5). Ki was determined from the measured Vmax using the equation:

$$Ki = [\text{PR} - \text{peptide}] / \{(Vm/Vapp) - 1\} \quad \text{Eq. 2}$$

Where, Vm is the maximum velocity achieved by the enzyme in the absence of inhibitors and Vapp is the maximum velocity achieved by the enzyme in the presence of a given concentration of PR-peptide, namely, [PR-peptide].

Cell culture experiments

VCAM-1 expression assay—Human umbilical vein endothelial cells (HUVECs, Cambrex Bio Science Walkersville, Inc) were cultured in endothelial cell basal medium-2 supplemented with EGM-2 SingleQuots (Cambrex) and 20%FBS. Confluent HUVECs, passaged 3–5 times, were starved overnight in medium supplemented with 0.5% FBS and 0.25% BSA. HUVECs, were exposed for 2 hours to TNF-α (0.25ng/ml) in the absence or presence of PR-peptides (1μM) as described by Gao et al. 10. Cells were then washed, lysed, and VCAM-1 immunoprecipitated. Following SDS-PAGE and membrane transfer of the immunoprecipitated sample, VCAM -1 expression was visualized by Western blotting with an anti VCAM-1 antibody (Santa-Cruz Biotechnology, Inc.) and normalized relative to actin (loading control).

NMR spectroscopy—One- and two-dimensional solution NMR spectra of PR11 and its alanine mutants were taken in PBS at 7 °C using an 800 MHz NMR Bruker Avance spectrometer fitted with a cryoprobe. The lower temperature was chosen to minimize thermal motion (conformational fluctuations) in peptides. Standard pulse programs available within the Bruker suite of experiments were used with optimization of pulse lengths and power levels. Two-dimensional NMR spectra were recorded in the phase sensitive mode using states-TPPI for quadrature detection in the t1 dimension30; 31. Solvent suppression

for NOESY and TOCSY experiments was achieved using excitation sculpting method with gradients32. TOCSY and NOESY spectra were referenced to water proton signal at 280 K. For TOCSY data, recorded using a MLEV-17 mixing scheme33, mixing times of 50 and 80 ms were used. NOESY experiments were carried out with 250, 400, and 600 ms; the latter was used in spin system identification and proton assignments. Two-dimensional data were collected with 2048 × 512 complex data points with 8 scans per increment and a spectral width of 10 ppm in each dimension. All data were processed using Felix (Accelrys Inc., San Diego, CA). Either a 60°-shifted sine-squared bell or, for resolution enhancement, a 30°-shifted sines-quared bell window function were applied in both dimensions, then zero-filled and Fourier transformed. Face-Lift34 base line correction method was applied to both dimensions. Sequence-specific assignments were made using established protocols35 and various site-specific mutants of PR11. Assignments of the first three residues were confirmed using alanine scanning mutations at these positions.

Supplementary Material

Refer to Web version on PubMed Central for supplementary material.

Acknowledgments

Initial samples of PR39, PR11, and AAA-PR11 were provided by MicroHeart Inc. Ms. Catherine Nguyen is acknowledged for her efforts at the initial stage of this project. The Keck-GCC 800 MHz NMR spectrophotometer of University of Houston was used in this work. We thank Dr. Filamon Tan and Mr. Julio Charles for access to fluorescence plate reader. SV thanks Drs. Lewis Kay and Dong-Sun Lee for efforts toward examining the conformation of PR11 bound to Thermoplasma 20S proteasome. This work was funded by the American Heart Association Beginning-Grant-in-Aid (SV), NIH (MS), and American Heart Association Scientist Development Grant (DT).

This work was partly supported by NIH grant #5R01HL053793-11 (MS), American Heart Association Beginning-Grant-in-Aid #0365134Y (SV) and American Heart Association Scientist Development Grant # 0635107N (DT).

References

1. Agerberth B, Gunne H, Odeberg J, Kogner P, Boman HG, Gudmundsson GH. PR-39, a proline-rich peptide antibiotic from pig, and FALL-39, a tentative human counterpart. Vet Immunol Immunopathol. 1996; 54:127–131. [PubMed: 8988856]
2. Agerberth B, Lee JY, Bergman T, Carlquist M, Boman HG, Mutt V, Jornvall H. Amino acid sequence of PR-39. Isolation from pig intestine of a new member of the family of proline-arginine-rich antibacterial peptides. Eur J Biochem. 1991; 202:849–854. [PubMed: 1765098]
3. Gallo RL, Ono M, Povsic T, Page C, Eriksson E, Klagsbrun M, Bernfield M. Syndecans, cell surface heparan sulfate proteoglycans, are induced by a proline-rich antimicrobial peptide from wounds. Proc Natl Acad Sci U S A. 1994; 91:11035–11039. [PubMed: 7972004]
4. Gudmundsson GH, Magnusson KP, Chowdhary BP, Johansson M, Andersson L, Boman HG. Structure of the gene for porcine peptide antibiotic PR-39, a cathelin gene family member: comparative mapping of the locus for the human peptide antibiotic FALL-39. Proc Natl Acad Sci U S A. 1995; 92:7085–7089. [PubMed: 7624374]
5. Li J, Post M, Volk R, Gao Y, Li M, Metais C, Sato K, Tsai J, Aird W, Rosenberg RD, Hampton TG, Sellke F, Carmeliet P, Simons M. PR39, a peptide regulator of angiogenesis. Nat Med. 2000; 6:49–55. [PubMed: 10613823]
6. Tirziu D, Chorianopoulos E, Moodie KL, Palac RT, Zhuang ZW, Tjwa M, Roncal C, Eriksson U, Fu Q, Elfenbein A, Hall AE, Carmeliet P, Moons L, Simons M. Myocardial hypertrophy in the absence of external stimuli is induced by angiogenesis in mice. J Clin Invest. 2007; 117:3188–3197. [PubMed: 17975666]
7. Li J, Brown LF, Laham RJ, Volk R, Simons M. Macrophagedependent regulation of syndecan gene expression. Circ Res. 1997; 81:785–796. [PubMed: 9351452]

8. Volk R, Schwartz JJ, Li J, Rosenberg RD, Simons M. The role of syndecan cytoplasmic domain in basic fibroblast growth factor-dependent signal transduction. J Biol Chem. 1999; 274:24417–24424. [PubMed: 10446222]
9. Bao J, Sato K, Li M, Gao Y, Abid R, Aird W, Simons M, Post MJ. PR-39 and PR-11 peptides inhibit ischemia-reperfusion injury by blocking proteasome-mediated I kappa B alpha degradation. Am J Physiol Heart Circ Physiol. 2001; 281:H2612–H2618. [PubMed: 11709430]
10. Gao Y, Lecker S, Post MJ, Hietaranta AJ, Li J, Volk R, Li M, Sato K, Saluja AK, Steer ML, Goldberg AL, Simons M. Inhibition of ubiquitin-proteasome pathway-mediated I kappa B alpha degradation by a naturally occurring antibacterial peptide. J Clin Invest. 2000; 106:439–448. [PubMed: 10930447]
11. Adams J, Kauffman M. Development of the proteasome inhibitor Velcade (Bortezomib). Cancer Invest. 2004; 22:304–311. [PubMed: 15199612]
12. Gaczynska M, Osmulski PA. Small-molecule inhibitors of proteasome activity. Methods Mol Biol. 2005; 301:3–22. [PubMed: 15917622]
13. Groll M, Berkers CR, Ploegh HL, Ovaa H. Crystal structure of the boronic acid-based proteasome inhibitor bortezomib in complex with the yeast 20S proteasome. Structure. 2006; 14:451–456. [PubMed: 16531229]
14. Ross JS, Schenkein DP, Pietrusko R, Rolfe M, Linette GP, Stec J, Stagliano NE, Ginsburg GS, Symmans WF, Pusztai L, Hortobagyi GN. Targeted therapies for cancer 2004. Am J Clin Pathol. 2004; 122:598–609. [PubMed: 15487459]
15. Jonzeiro CAP, Anderson KC, Hunter T. Proteasome inhibitor drugs on the rise. Cancer Research. 2006; 66:7840–7842. [PubMed: 16861477]
16. Adams J, Behnke M, Chen S, Cruickshank AA, Dick LR, Grenier L, Klunder JM, Ma YT, Plamondon L, Stein RL. Potent and selective inhibitors of the proteasome: dipeptidyl boronic acids. Bioorg Med Chem Lett. 1998; 8:333–338. [PubMed: 9871680]
17. Teicher BA, Ara G, Herbst R, Palombella VJ, Adams J. The proteasome inhibitor PS-341 in cancer therapy. Clin Cancer Res. 1999; 5:2638–2645. [PubMed: 10499643]
18. Unno M, Mizushima T, Morimoto Y, Tomisugi Y, Tanaka K, Yasuoka N, Tsukihara T. The structure of the mammalian 20S proteasome at 2.75 A resolution. Structure (Camb). 2002; 10:609–618. [PubMed: 12015144]
19. Groll M, Ditzel L, Lowe J, Stock D, Bochtler M, Bartunik HD, Huber R. Structure of 20S proteasome from yeast at 2.4 A resolution. Nature. 1997; 386:463–471. [PubMed: 9087403]
20. Gaczynska M, Osmulski PA, Gao Y, Post MJ, Simons M. Proline- and arginine-rich peptides constitute a novel class of allosteric inhibitors of proteasome activity. Biochemistry. 2003; 42:8663–8670. [PubMed: 12873125]
21. Brandts JF, Halvorson HR, Brennan M. Consideration of the Possibility that the slow step in protein denaturation reactions is due to cis-trans isomerism of proline residues. Biochemistry. 1975; 14:4953–4963. [PubMed: 241393]
22. Garel J-R, Baldwin RL. Both the Fast and Slow Refolding Reactions of Ribonuclease A Yield Native Enzyme. Proceedings of the National Academy of Sciences (United States of America). 1973; 70:3347–3351.
23. MacArthur MW, Thornton JM. Influence of proline residues on protein conformation. J Mol Biol. 1991; 218:397–412. [PubMed: 2010917]
24. Taylor CM, Hardre R, Edwards PJ, Park JH. Factors affecting conformation in proline-containing peptides. Org Lett. 2003; 5:4413–4416. [PubMed: 14602013]
25. Zanetti M, Gennaro R, Gallo RL. Anti-microbial activity and cell binding are controlled by sequence determinants in the anti-microbial peptide PR-39. J Invest Dermatol. 2001; 116:230–235. [PubMed: 11179998]
26. Chan YR, Gallo RL. PR-39, a syndecan-inducing antimicrobial peptide, binds and affects p130(Cas). J Biol Chem. 1998; 273:28978–28985. [PubMed: 9786902]
27. Pando MP, Verma IM. Signal-dependent and -independent degradation of free and NF-kappa B-bound IkappaBalpha. J Biol Chem. 2000; 275:21278–21286. [PubMed: 10801847]

28. Croy CH, Bergqvist S, Huxford T, Ghosh G, Komives EA. Biophysical characterization of the free IkappaBalpha ankyrin repeat domain in solution. Protein Sci. 2004; 13:1767–1777. [PubMed: 15215520]

29. Smith DM, Chang SC, Park S, Finley D, Cheng Y, Goldberg AL. Docking of the proteasomal ATPases' carboxyl termini in the 20S proteasome's alpha ring opens the gate for substrate entry. Mol Cell. 2007; 27:731–744. [PubMed: 17803938]

30. Marion D, Wuthrich K. Application of Phase Sensitive Two- Dimensional Correlated Spectroscopy (Cosy) for Measurements of H-1-H-1 Spin-25 Spin Coupling-Constants in Proteins. Biochemical and Biophysical Research Communications. 1983; 113:967–974. [PubMed: 6307308]

31. Redfield AG, Kunz SD. Quadrature Fourier Nmr Detection - Simple Multiplex for Dual Detection and Discussion. Journal Magnetic Resonance. 1975; 19:250–254.

32. Hwang TL, Shaka AJ. Water Suppression That Works - Excitation Sculpting Using Arbitrary Wave-Forms and Pulsed-Field Gradients. Journal Magnetic Resonance. 1995; 112:275–279.

33. Bax A, Davis DG. Mlev-17-Based Two-Dimensional Homonuclear Magnetization Transfer Spectroscopy. Journal Magnetic Resonance. 1985; 65:355–360.

34. Chylla RA, Markley JL. Simultaneous Basepoint Correction and Signal Recognition in Multidimensional Nmr-Spectra. Journal of Magnetic Resonance Series B. 1993; 102:148–154.

35. Wuthrich, K. NMR of proteins and nucleic acids. First edit. John Wiley & Sons, Inc.; 1986.

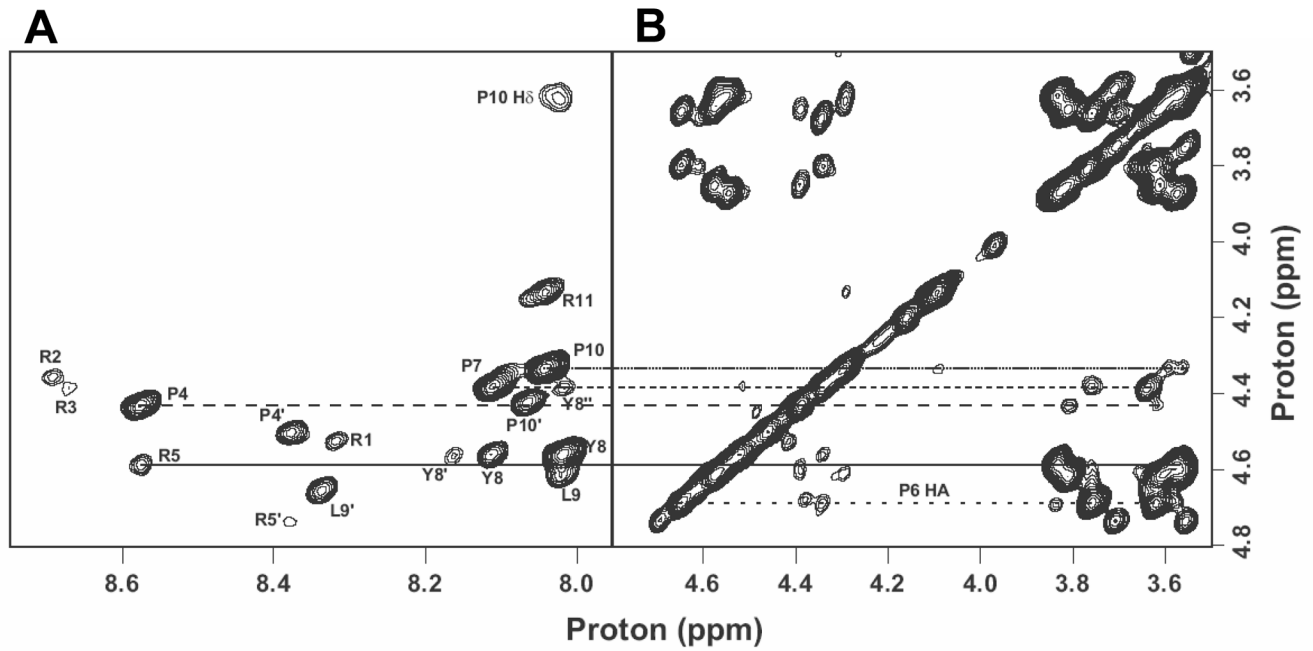

Figure 1. Homonuclear NOESY spectrum of PR11

Left. Finger print region identifying sequence-specific assignments and correlations to backbone amide protons.

Right. Cross peaks originating from side chain protons.

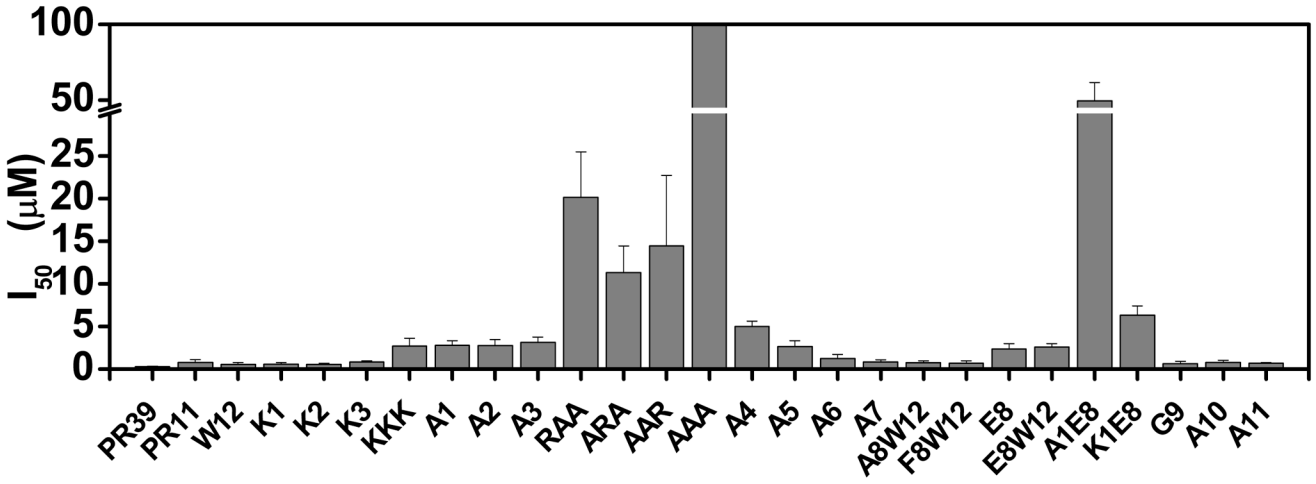

Figure 2. Inhibition of chymotrypsin-like activity of 20 S proteasome by PR-peptides

The ability of PR11 and its mutants to inhibit the chymotrypsin-like activity of mammalian 20S proteasomes were assayed. Relative activities of the proteasome in the presence of various PR-peptides were assessed from the concentrations of the fluorescent methylcoumaramide (MCA) product.

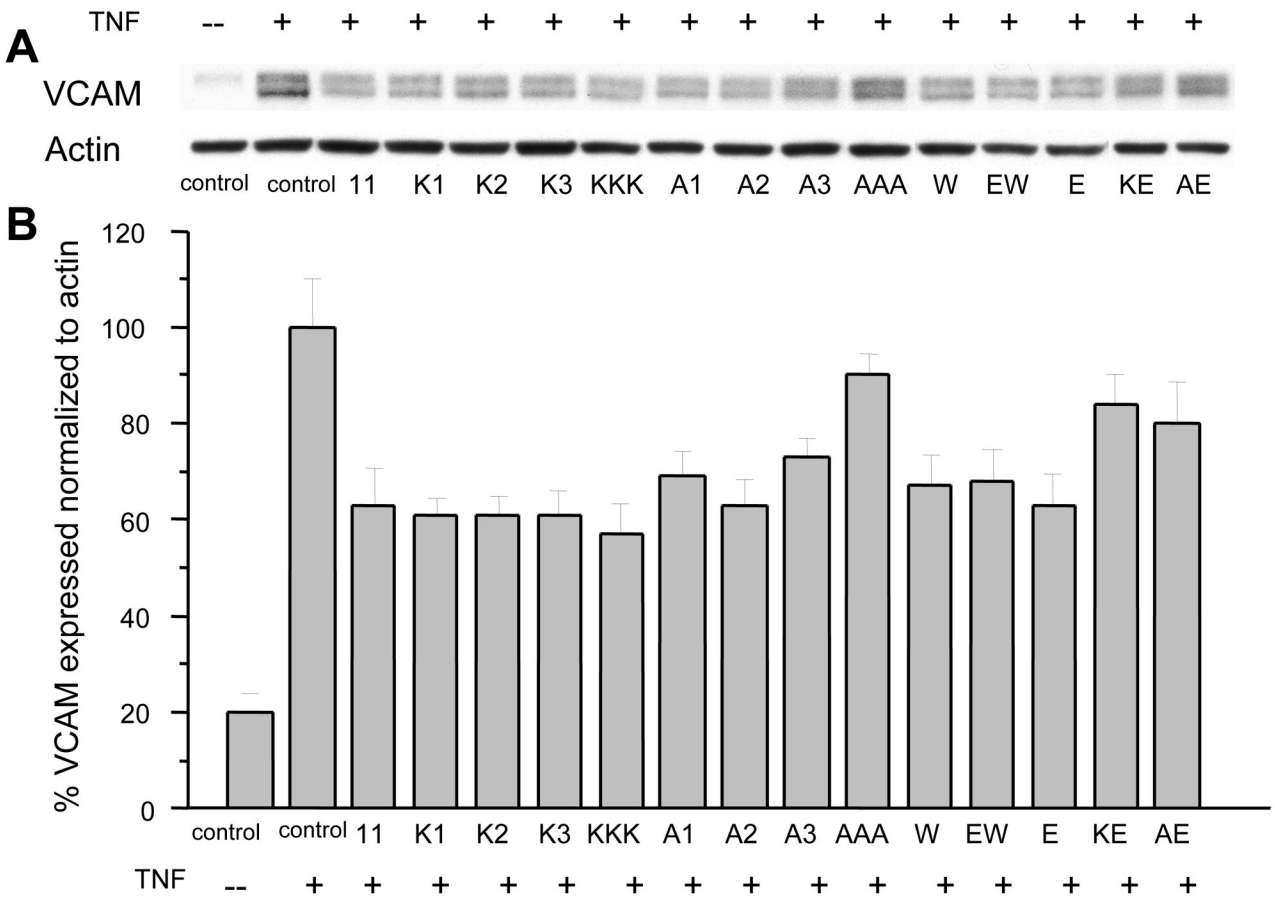

Figure 3. VCAM-1 expression was evaluated in TNF-α-activated (+) human umbilical vein endothelial cells (HUVECs) in the absence or presence of PR11 or its mutants

(A) Western Blots identify the expression of VCAM-1 expression and that of actin. **(B)** Plot of VCAM-1 expression levels normalized relative to actin.

Table I

Proton Chemical Shift Assignments for PR11[a]

Residue	NH	H_α	H_β	Other
ARG1	8.31	3.79	1.81	γCH2, 1.64; δCH2
ARG2	8.69	4.37	1.81	γCH2, 1.68, 1.65; δCH2, 3.23
ARG3	8.67	4.62	1.87	γCH2, 1.76; δCH2, 3.25
PRO4		4.44	2.31, 2.04	γCH2, 1.88; δCH2, 3.86, 3.67
ARG5	8.58	4.58	1.84	γCH2, 1.74; δCH2, 3.22
PRO6		4.69	2.36, 2.04	γCH2, 1.81; δCH2, 3.88, 3.62
PRO7		4.39	2.27, 2.02	γCH2, 2.11; δCH2, 3.81, 3.67
TYR8	8.09	4.56	3.06, 2.97	δCH2, 7.13; εCH2, 6.84
LEU9	8.02	4.62	1.51	γCH, 1.51*; δCH3, 0.91
PRO10		4.35	2.31, 2.04	γCH2, 1.98; δCH2, 3.64, 3.60
ARG11	8.04	4.14	1.85	γCH2, 1.74, 1.64; δCH2, 3.21

[a]Experimental conditions: PBS, pH 7.40, 280 K

*Ambiguous assignment

Table II

Human 20S proteasome inhibitory activities of PR39 and its mutants (Arranged in the order of increasing I50 values)

Peptide	Sequence	I50[a](μM)	error[b]	N[c]	error[b]
PR39	RRRPRPPYLPRPRPPPFFPPRLPPRIPPGFPPRFPPRFP	0.004	0.005	1.232	0.151
W12	RRRPRPPYLPR**W**	0.006	0.019	1.171	0.161
F8W12	RRRPRPP**F**LPR**W**	0.034	0.060	1.128	0.153
G9	RRRPRPPY**G**PR	0.137	0.116	1.389	0.319
K2	R**K**RPRPPYLPR (K2)	0.543	0.156	1.093	0.264
K1	**K**RRRPPYLPR (K1)	0.595	0.186	0.933	0.258
A11	RRRPRPPYLP**A**	0.685	0.119	1.953	0.305
A8W12	RRRPRPP**A**LPR**W** (A8W12)	0.715	0.267	1.154	0.310
A10	RRRPRPPYL**A**R	0.782	0.231	1.321	0.292
PR11	RRRPRPPYLPR (**wild type**)	0.805	0.321	0.977	0.248
K3	RR**K**PRPPYLPR (K3)	0.819	0.154	1.150	0.226
A7	RRRPRP**A**YLPR	0.851	0.220	3.921	1.259
A6	RRRPR**A**PYLPR	1.223	0.485	2.804	1.145
E8	RRRPRPP**E**LPR (E8)	2.373	0.632	1.341	0.290
E8W12	RRRPRPP**E**LPR**W** (E8W12)	2.615	0.369	2.568	0.297
A5	RRRP**A**PPYLPR	2.652	0.691	3.489	0.813
KKK	**KKK**PRPPYLPR (KKK)	2.714	0.916	1.177	0.337
A2	R**A**RPRPPYLPR (A2)	2.767	0.709	1.636	0.330
A1	**A**RRPRPPYLPR (A1)	2.811	0.507	1.722	0.258
A3	RR**A**PRPPYLPR (A3)	3.153	0.600	1.900	0.277
A4	RRR**A**RPPYLPR	4.993	0.653	1.769	0.151
K1E8	**K**RRPRPPELPR (K1E8)	6.336	1.073	1.586	0.162
ARA	**ARA**PRPPYLPR	11.299	3.150	1.598	0.164
AAR	**AA**RPRPPYLPR	14.479	8.268	1.663	0.328
RAA	R**AA**PRPPYLPR	20.130	0.122	1.447	0.122
A1E8	**A**RRPRPP**E**LPR (A1E8)	49.448	12.039	2.179	0.450
AAA	**AAA**PRPPYLPR (AAA)	>100	N/A	N/A	N/A

[a]I50 corresponds to the concentration of PR-peptide required for half maximal inhibition.

[b] Error is standard deviation obtained by non-linear least-squares curve-fitting of 20S proteasome activity plotted as a function of PR-peptide concentration (Eq. 1).

[c] N corresponds to fractional occupation of PR-peptide on 20S proteasome, derived from curve-fitting procedures.

Table III

Inhibition constants of PR11 and some its most active mutants.

Peptide	Ki (nM)	Error
PR11 (wild type)	86.5	21.1
W12	39.5	2.3
F8W12	184	16.3
A8W12	50.7	16.8

Conditions: 5 nM human 20S proteasome, 20–100 μM Suc-LLVY-AMC substrate, 0, 75 or 100 nM PR-peptide, 25 mM Tris, pH 7.5, 0.03% SDS, 37 °C. Under these conditions, Km for the enzyme was 47.4±5 μM and Vmax was 0.55±0.03 μmol/h/mg.